

Dehydrogenative Oligomerization of PhSiH₃ Catalyzed by (1-Me-Indenyl)Ni(PR₃)(Me)

Frédéric-Georges Fontaine and Davit Zargarian*

Département de Chimie, Université de Montréal, Montréal (Québec), Canada, H3C 3J7

Received August 17, 2001

The complexes (1-Me-Ind)Ni(PR₃)Me (Ind = indenyl; R = Ph, **1**; Cy, **2**; Me, **3**) can act as single-component precatalysts for the dehydrogenative oligomerization of PhSiH₃ to (PhSiH)_n with M_w up to 1.6×10^3 in the case of **3**. The catalytic Si–Si bond formation is initiated by a second-order, concerted reaction between the Ni–Me precursor and PhSiH₃ which releases CH₄. Kinetic studies of this Si–H bond activation step gave the following activation parameters for the reaction of **3** with PhSiH₃: $\Delta H^\ddagger = 10.7 \pm 0.7$ kcal·mol⁻¹; $\Delta S^\ddagger = -42 \pm 2$ eu; k_H/k_D (for reaction with PhSiD₃ at 313 K) = 9.8 ± 0.5 . The Ni–SiPhH₂ species presumed to form in this reaction was not detected directly, but the presence of 1-SiPhH₂-3-Me-Ind in the reaction mixtures, coupled with the fact that Ni(PMe₃)₄ is an active precatalyst for the oligomerization of PhSiH₃, suggests that the silyl intermediate undergoes a reductive elimination to generate Ni(0) species which might be involved in the catalysis.

Introduction

The search for new synthetic routes to polysilanes (R–Si–R')_n is driven by the potential of these materials in microlithography, photoconduction, electroluminescence, the fabrication of optical devices, and as precursors to silicon carbide.¹ The discovery² and development³ of effective, transition-metal-based routes for the dehydrogenative coupling of silanes has provided an interesting alternative to the traditional Wurtz coupling of halosilanes for the synthesis of these catenated polymers. The most promising catalysts reported to date are some derivatives of group 4 metallocenes,³ but recent reports have shown that a number of other systems can be effective for silane polymerization. For instance, Pt-(COD)₂ can polymerize⁴ secondary silanes such as Et₂-SiH₂ to Si-containing polymers of relatively high M_w , while M(CO)₆ (M = Cr, Mo, W) can dehydrocouple the tertiary Si–H bonds in poly(methylsilene), (–Si(H)(Me)–CH₂–)_n, to produce cross-linked preceramic materials.⁵

In this context, we have reported that PhSiH₃ can be polymerized to (PhSiH)_n having M_w in the range of (2–7) × 10³ by a system consisting of the complex (1-Me-Ind)Ni(PPh₃)Cl (Ind = indenyl) and methylaluminumoxane (MAO).⁶ This system was initially thought to operate

via a cationic mechanism involving an intermediate of the type [(1-Me-Ind)Ni(PPh₃)⁺]; later studies indicated, however, that the catalysis involves neutral Ni–Me derivatives formed in situ by the methylation of the Ni–Cl precursor with MAO. This finding prompted us to examine the reaction of PhSiH₃ with a number of preformed Ni–Me derivatives in an attempt to better understand their role in the Ni/MAO-catalyzed polymerization of PhSiH₃. Herein we report the results of our mechanistic studies on the dehydrocoupling of PhSiH₃ by the complexes (1-Me-Ind)Ni(PR₃)Me (R = Ph, **1**; Cy, **2**; Me, **3**).

Experimental Section

General Comments. All manipulations were performed under an inert atmosphere of N₂ or argon using standard Schlenk techniques and a drybox. Dry, oxygen-free solvents were employed throughout. The preparation and complete characterization of complex **1**⁷ and the Ni–Cl precursors⁸ to **2** and **3** have been reported previously. PhSiH₃ and all other reagents used in the experiments were obtained from commercial sources and used as received. The elemental analyses were performed by the Laboratoire d'analyse élémentaire (Université de Montréal). The NMR spectra were recorded using the following spectrometers: Bruker DMX600 (2D ¹H–²⁹Si), Bruker AMX400 (¹H at 400 MHz, ¹³C{¹H} at 100.56 MHz, and ³¹P{¹H} at 161.92 MHz), and Bruker AV300 (¹H at 300 MHz for TOCSY).

(1-Me-Ind)Ni(PCy₃)Me (2). MeLi (1.94 mL of a 1.4 M solution in Et₂O, 2.72 mmol) was added dropwise to a solution of (1-Me-Ind)Ni(PCy₃)Cl (912 mg, 1.81 mmol) in Et₂O (100 mL) and stirred for 2 h. Deoxygenated water (0.3 mL) was then added and stirred for 5 min. Drying over MgSO₄ followed by filtration and evaporation gave a dark powder (655 mg, crude yield 75%), which was recrystallized from cold Et₂O to give red crystals suitable for X-ray diffraction studies. ¹H NMR

(1) (a) West, R. *J. Organomet. Chem.* **1986**, *300*, 327. (b) Miller, R. D.; Michl, J. *Chem. Rev.* **1989**, *89*, 1359.

(2) Aitken, C.; Harrod, J. F.; Samuel, E. *J. Organomet. Chem.* **1985**, *279*, C11.

(3) For a few leading references see: (a) Tilley, T. D. *Acc. Chem. Res.* **1993**, *26*, 22. (b) Harrod, J. F.; Mu, Y.; Samuel, E. *Polyhedron* **1991**, *10*, 1239. (c) Shaltout, R. M.; Corey, J. Y. *Organometallics* **1996**, *15*, 2866. (d) Campbell, W. H.; Hilty, T. K.; Yurga, L. *Organometallics* **1989**, *8*, 2615. (e) Banovetz, J. P.; Stein, K. M.; Waymouth, R. M. *Organometallics* **1991**, *10*, 3430. (f) Hengge, E.; Gspaltl P.; Pinter, E. *J. Organomet. Chem.* **1996**, *521*, 145. (g) Choi, N.; Onozawa, S.; Sakakura, T.; Tanaka, M. *Organometallics* **1997**, *16*, 2765.

(4) Chaunan, B. P. S.; Shimizu, T.; Tanaka, M. *Chem. Lett.* **1997**, 785.

(5) Yang, S. Y.; Park, J. M.; Woo, H. G.; Kim, W. G.; Kim, I. S.; Kim, D. P.; Hwang, T. S. *Bull. Korean Chem. Soc.* **1997**, *12*, 1264.

(6) Fontaine, F.-G.; Kadkhodazadeh, T.; Zargarian, D. *J. Chem. Soc., Chem. Commun.* **1998**, 1253.

(7) Huber, T. A.; Bayrakdarian, M.; Dion, S.; Dubuc, I.; Bélanger-Gariépy, F.; Zargarian, D. *Organometallics* **1997**, *16*, 5811.

(8) Fontaine, F.-G.; Dubois, M.-A.; Zargarian, D. *Organometallics* **2001**, *20*, 5156.

(C₆D₆): δ 7.20–7.16 and 7.01–6.95 (m, aromatic protons of Ind), 6.26 (d, $^3J_{\text{H-H}} = 3.0$, H2), 4.73 (b, H3), 1.90 (d, $^4J_{\text{P-H}} = 3.5$, 1-CH₃-Ind), 1.80–1.00 (m, PCy₃), –0.86 (d, $^3J_{\text{P-H}} = 4.5$, Ni-CH₃). ¹³C{¹H} NMR (C₆D₆): 124.1 (s, C3a or C7a), 123.5 (s, C3a or C7a), 122.3 (s, C5 or C6), 121.4 (s, C5 or C6), 118.0 (s, C4 or C7), 116.1 (s, C4 or C7), 102.6 (s, C2), 87.0 (d, $^2J_{\text{P-C}} = 11.2$, C1), 69.3 (s, C3), 35.8 (d, $^1J_{\text{P-C}} = 20.1$, P-CH), 30.1 (d, $^2J_{\text{P-C}} = 24.8$, PCH(CH₂CH₂)₂CH₂), 27.9 (d, $^3J_{\text{P-C}} = 11.2$, PCH(CH₂CH₂)₂CH₂), 26.8 (s, PCH(CH₂CH₂)₂CH₂), 10.7 (d, $^3J_{\text{P-C}} = 1.6$, CH₃-Ind), –22.7 (d, $^2J_{\text{P-C}} = 23.3$, Ni-CH₃). ³¹P{¹H} NMR (C₆D₆): 48.29 (s). Anal. Calcd for C₂₉H₄₅NiP₁: C, 72.06; H, 9.38. Found: C, 71.64; H, 9.73.

(1-Me-Ind)Ni(PMe₃)Me (3). MeLi (1.07 mL of a 1.4 M solution in Et₂O, 1.5 mmol) was added dropwise to a solution of (1-Me-Ind)Ni(PMe₃)Cl (300 mg, 1.00 mmol) in Et₂O (30 mL). The solution was stirred for 30 min, and then deoxygenated water (1 mL) was added and stirred for 5 min. Drying over MgSO₄ followed by filtration and evaporation gave a dark red powder (128 mg, 53% yield). Recrystallization from cold hexanes gave suitable crystals (dark red) for X-ray diffraction studies. ¹H NMR (C₆D₆): δ 7.16 (br d, $^3J_{\text{H-H}} = 8.0$, H4 or H7), 7.06 (pseudo td, $^3J_{\text{H-H}} = 7.8$, $^4J_{\text{H-H}} = 1.6$, H5 or H6), 7.00 (pseudo td, $^3J_{\text{H-H}} = 7.7$, $^4J_{\text{H-H}} = 1.2$, H5 or H6), 7.16 (br d, $^3J_{\text{H-H}} = 7.6$, H4 or H7), 6.07 (d, $^3J_{\text{H-H}} = 2.0$, H2), 4.44 (b, H3), 1.95 (d, $^4J_{\text{P-H}} = 3.7$, CH₃-Ind), 0.63 (d, $^2J_{\text{P-H}} = 9.1$, P-CH₃), –0.78 (d, $^3J_{\text{P-H}} = 6.2$, Ni-CH₃). ¹³C{¹H} NMR (C₆D₆): 121.9 (s, C5 or C6), 121.8 (s, C5 or C6), 121.5 (s, C3a or C7a), 120.6 (s, C3a or C7a), 116.2 (s, C4 or C7), 116.1 (s, C4 or C7), 101.7 (s, C2), 88.3 (d, $^2J_{\text{P-C}} = 12.0$, C1), 69.4 (s, C3), 16.1 (d, $^1J_{\text{P-C}} = 27.3$, P-CH₃), 10.8 (d, $^3J_{\text{P-C}} = 1.6$, CH₃-Ind), –20.7 (d, $^2J_{\text{P-C}} = 24.1$, Ni-CH₃). ³¹P{¹H} NMR (C₆D₆): –3.72 (s). Anal. Calcd for C₁₄H₂₁NiP₁: C, 60.27; H, 7.59. Found: C, 60.14; H, 7.72.

Crystal Structure Determinations. Suitable crystals of **2** and **3** were attached to glass fibers and transferred rapidly and under a cold stream of nitrogen to an Enraf-Nonius CAD-4 diffractometer equipped with a low-temperature gas stream cryostat for data collection at 220(2) K. The data were collected with graphite-monochromated Cu K α radiation; the refinement of the cell parameters was done using the CAD-4 software⁹ on 25 reflections, while NRC-2 and NRC-2A were used for the data reduction.¹⁰ Both structures were solved by direct methods using SHELXS96,¹¹ and the refinements were done on F^2 by full-matrix least squares. All non-hydrogen atoms were refined anisotropically, while the hydrogens (isotropic) were constrained to the parent atom using a riding model. Crystal data and experimental details for both compounds are listed in Table 1 and selected bond distances and angles are listed in Table 2. The complete crystallographic reports are included in the Supporting Information.

Catalytic Studies. The catalytic experiments were carried out by stirring 3–5 mg of each precatalyst in ca. 200 mg of PhSiH₃ (ca. 200 equiv) under an inert atmosphere. The resulting oil or solid product was dissolved in THF, passed through a microfilter, and analyzed by a Waters GPC system equipped with a refractive index detector calibrated with polystyrene standards in THF. (Note: Care should be taken not to expose these samples to air prior to analysis.)¹² As in

Table 1. Crystal Data, Data Collection, and Structure Refinement of **2 and **3****

	2	3
formula	C ₂₉ H ₄₅ Ni P	C ₁₄ H ₂₁ NiP
mol wt	483.330	278.988
cryst color	clear red	dark red
cryst habit	plate	block
cryst dimens, mm	0.08 × 0.24 × 0.20	0.23 × 0.19 × 0.16
symmetry	monoclinic	orthorhombic
space group	$P2_1/n$	$P2_12_12_1$
<i>a</i> , Å	13.052(7)	7.685(3)
<i>b</i> , Å	14.345(6)	11.990(5)
<i>c</i> , Å	14.620(11)	15.230(5)
α , deg	90	90
β , deg	106.98(5)	90
γ , deg	90	90
volume, Å ³	2618(3)	1403.3(9)
<i>Z</i>	4	4
<i>D</i> (calcd), g cm ^{–3}	1.2263	1.3205
diffractometer	Nonius CAD-4	Nonius CAD-4
temp, K	220(2)	220(2)
λ (Cu K α), Å	1.54056	1.54056
μ , mm ^{–1}	1.723	2.825
scan type	$\omega/2\theta$ scan	$\omega/2\theta$ scan
θ_{max} , deg	69.84	69.87
<i>h, k, l</i> range	–15 ≤ <i>h</i> ≤ 15 –17 ≤ <i>k</i> ≤ 17 0 ≤ <i>l</i> ≤ 17	–9 ≤ <i>h</i> ≤ 9 –14 ≤ <i>k</i> ≤ 14 –18 ≤ <i>l</i> ≤ 18
no. of refls used (<i>I</i> > 2 σ (<i>I</i>))	4916	2668
abs corr	integration	integration
<i>T</i> (max, min)	0.89 and 0.69	0.72 and 0.55
$R[F^2 > 2\sigma(F^2)]$, $wR(F^2)$	0.0558, 0.1365	0.0346, 0.0754
GOF	0.937	0.915

Table 2. Selected Bond Distances (Å) and Angles (deg) for **1–3**

	1	2	3
Ni–P	2.1213(13)	2.1710(13)	2.1239(11)
Ni–C(9)	1.991(3)	1.965(4)	1.955(3)
Ni–C(1)	2.089(4)	2.104(4)	2.097(3)
Ni–C(2)	2.072(4)	2.071(4)	2.076(3)
Ni–C(3)	2.082(4)	2.110(4)	2.095(3)
Ni–C(3A)	2.275(4)	2.321(3)	2.298(3)
Ni–C(7A)	2.273(4)	2.320(3)	2.288(3)
C(1)–C(2)	1.407(5)	1.410(6)	1.409(5)
C(2)–C(3)	1.404(5)	1.411(5)	1.410(4)
C(3)–C(3A)	1.430(5)	1.457(5)	1.445(5)
C(3A)–C(7A)	1.424(5)	1.421(5)	1.435(4)
C(1)–C(7A)	1.438(3)	1.460(5)	1.451(5)
$\Delta\text{M–C}^a$	0.19	0.21	0.20
P–Ni–C(9)	99.51(10)	96.05(11)	93.30(10)
C(3)–Ni–C(9)	159.84(16)	158.05(15)	163.19(12)
C(3)–Ni–P	104.04(13)	105.76(11)	103.25(9)
C(1)–Ni–C(9)	94.26(16)	92.05(16)	97.40(13)
C(1)–Ni–P	170.22(13)	171.31(11)	168.34(10)
C(1)–Ni–C(3)	66.19(16)	66.04(15)	66.37(13)

^a See ref 17 for the definition of $\Delta\text{M–C}$ and literature values for other indenyl complexes.

the case of most (PhSiH)_{*n*} samples obtained from transition-metal-catalyzed reactions, the products of these catalytic reactions displayed broad ¹H NMR signals characteristic of linear (4.4–4.8 ppm) and cyclic (5.2–6.0 ppm) oligomers.¹³ The gel permeation chromatograms of these samples also display two distinct, and often overlapping, peaks that represent the linear and cyclic components of the mixture. The ratios of the two Si-H signals in the ¹H NMR spectra are similar to the ratio of the peak areas in the GPC runs. It should be noted that according to Harrod et al. the molecular weights of (PhSiH)_{*n*} determined from the GPC runs versus polystyrene standards are often underestimated.¹⁴ The values presented

(13) (a) Woo, H.-G.; Walzer, J. F.; Tilley, T. D. *J. Am. Chem. Soc.* **1992**, *114*, 7047. (b) Gauvin, F. Ph.D. Thesis, McGill University, 1992.

(9) CAD-4 Software, version 5.0; Enraf-Nonius: Delft, The Netherlands, 1989.

(10) Gabe, E. J.; Le Page, Y.; Charlant, J.-P.; Lee, F. L.; White, P. S. *J. Appl. Crystallogr.* **1989**, *22*, 384.

(11) Sheldrick, G. M. *SHELXL96*, Program for the Solution of Crystal Structures; University of Göttingen: Germany, 1990.

(12) (a) According to a recent study (ref 12b), samples of (PhSiH)_{*n*} are only partially oxidized even after being exposed to air for 12 h in refluxing xylene. We have found, however, that the samples obtained from our Ni-catalyzed reactions are very air-sensitive even at ambient temperature. It is not clear whether this apparently increased air-sensitivity of our polysilane samples is due to the presence of trace amounts of Ni particles left over from the catalytic reactions. (b) Chatgililoglu, C.; Guerrini, A.; Lucarini, M.; Pedulli, G. F.; Carrozza, P.; Da Riot, G.; Borzatta, V.; Lucchini, V. *Organometallics* **1998**, *17*, 2169.

in this report have not been corrected for such a systematic error.

Kinetic Studies. The kinetic studies were carried out as follows. A Wilmad 528-TR-7 screwcap NMR tube containing 0.7 mL of a 0.02 M C₆D₆ solution of the precatalysts was heated to the desired temperature inside the NMR instrument's probe prior to the injection (via the septum) of PhSiH₃ (50, 70, or 90 equiv) and a precisely measured amount of toluene as internal standard. The progress of each reaction was monitored by following the disappearance of the Ni-CH₃ and the Ind-CH₃ signals of the precatalyst by ¹H NMR spectroscopy. It should be noted that we used the data obtained up to one half-life because the data obtained after prolonged reaction times caused deviations from linearity. The nonlinear kinetic behavior is attributed to the secondary reactions of PhSiH₃ with the intermediates arising from the initial reaction with the precatalysts (vide infra).

Results

Synthesis and Characterization of the Complexes. Complexes **2** and **3** were obtained in 50–75% yields by reacting the Ni-Cl precursors with MeLi in analogy with the synthesis of **1**.⁷ In solution, these complexes are air sensitive but thermally stable; in the solid state they are stable to air for a few days. The spectroscopic characterization of these complexes was quite straightforward: the ³¹P{¹H} NMR spectra showed the expected^{7,8,15} singlet resonances (48.3 and –3.7 ppm for **2** and **3**, respectively), while the ¹H and ¹³C{¹H} NMR spectra contained the upfield signals characteristic of the Ni-Me moieties (¹H: ca. –0.8 ppm, ³J_{P-H} = 4.5 for **2** and 6.2 for **3**; ¹³C{¹H}: –22.7 and –20.7 ppm, ²J_{P-C} = 23.3 and 24.1 Hz for **2** and **3**, respectively). Significantly, the ¹H NMR signals for Ind-CH₃ and H3 protons appeared downfield of the corresponding signals in the Ni-Cl analogues, thus confirming the increased η^5 hapticity of the Ind ligand upon methylation (vide infra).

The results of the X-ray studies (ORTEP diagrams in Figures 1 and 2) showed that the overall geometry around the Ni atom in complexes **2** and **3** is approximately square planar, with the largest distortion arising from the small C1–Ni–C3 angle of ca. 66°. The Ni–CH₃ distance is similar in both complexes (ca. 1.956(4) Å) and somewhat shorter than the corresponding distance in complex **1** (1.991(3) Å); on the other hand, the Ni–P distance is longer in complex **2** (2.1710(13) Å) relative to both **3** (2.1239(11) Å) and **1** (2.1213(13) Å) presumably because of the much larger cone angle of PCy₃. The large steric bulk of PCy₃ is also reflected in the slightly longer Ni–C(Ind) bonds.

As observed in the structures of the previously reported examples of this family of complexes,^{7,8,15} the 1-Me-Ind ligand in both **2** and **3** is bound to the Ni center primarily through the C1, C2, and C3 atoms (ca. 2.07–2.10 Å), whereas the Ni–C3a and Ni–C7a distances are significantly longer (ca. 2.29 and 2.32 Å). This

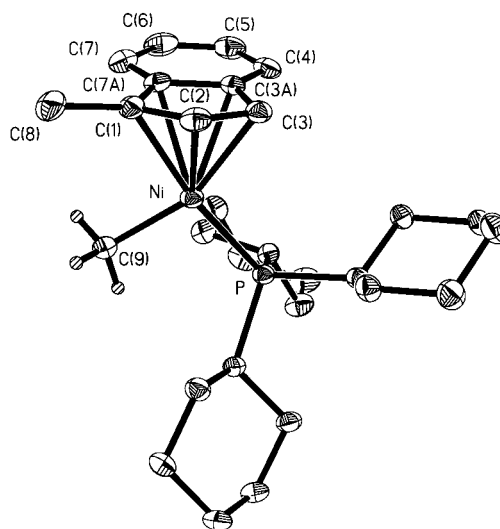


Figure 1. ORTEP diagram for complex **2** showing 30% probability thermal ellipsoids and the atom-numbering scheme.

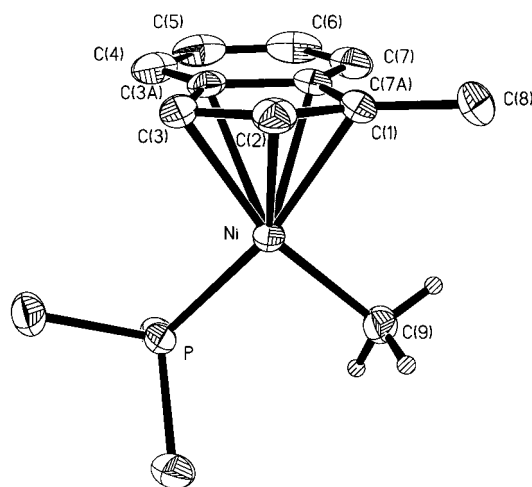


Figure 2. ORTEP diagram for complex **3** showing 30% probability thermal ellipsoids and the atom-numbering scheme.

kind of $\eta^5 \leftrightarrow \eta^3$ “slippage” can be attributed to the tendency of a d⁸ center to avoid forming an 18-electron complex.¹⁶ The parameter $\Delta M-C = \{M-C_{av} \text{ (for C3a and C7a)} - M-C_{av} \text{ (for C1 and C3)}\}$ is often used to measure the extent to which Ind ligands have slipped away from the idealized η^5 hapticity wherein $\Delta M-C$ should be nearly zero.¹⁷ The $\Delta Ni-C$ values for **2** (0.21 Å) and **3** (0.20 Å) are slightly larger than those observed for complex **1** (0.19 Å), probably reflecting the stronger nucleophilicity of tri(alkyl) phosphines. Comparison of the bonding parameters in these Ni-Me complexes and their Ni-Cl analogues^{7,8} reveals that (a) the degree of slippage is lower in the Ni-Me derivatives ($\Delta Ni-C = 0.25\text{--}0.30$ for Ni-Cl derivatives), and (b) the coordination of the 1-Me-Ind to the Ni center is symmetrical in

(14) Dioumaev V. K.; Harrod J. F. *Organometallics* **1994**, *13*, 1548.

(15) (a) Huber, T. A.; Bélanger-Gariépy, F.; Zargarian, D. *Organometallics* **1995**, *14*, 4997. (b) Bayraktarian, M.; Davis, M. J.; Reber, C.; Zargarian, D. *Can. J. Chem.* **1996**, *74*, 2194. (c) Vollmerhaus, R.; Bélanger-Gariépy, F.; Zargarian, D. *Organometallics* **1997**, *16*, 4762. (d) Dubuc, I.; Dubois, M.-A.; Bélanger-Gariépy, F.; Zargarian, D. *Organometallics* **1999**, *18*, 30. (e) Wang, R.; Bélanger-Gariépy, F.; Zargarian, D. *Organometallics* **1999**, *18*, 5548. (f) Groux, L. F.; Bélanger-Gariépy, F.; Zargarian, D.; Vollmerhaus, R. *Organometallics* **2000**, *19*, 1507.

(16) For a detailed discussion of hapticity issues in the corresponding CpNi complexes see: Holland, P. L.; Smith, M. E.; Andersen, R. A.; Bergman, R. G. *J. Am. Chem. Soc.* **1997**, *119*, 12815.

(17) For a discussion of the correlations between the solid-state and solution hapticities for indenyl complexes, on one hand, and the $\Delta M-C$ values and the ¹³C NMR data, on the other, see: (a) Baker, R. T.; Tulip, T. H. *Organometallics* **1986**, *5*, 839. (b) Westcott, S. A.; Kakkar, A. K.; Stringer, G.; Taylor, N. J.; Marder, T. B. *J. Organomet. Chem.* **1990**, *394*, 777.

Table 3. Dehydropolymerization of PhSiH₃ Using (1-Me-Ind)Ni(PR₃)Me

run	cat.	solvent	time (days)	T (°C)	% conv ^a	total mixture ^b			linear portion ^b			% lin ^c
						M _w	M _n	M _w /M _n	M _w	M _n	M _w /M _n	
1	1	neat	6	25	83				530	426	1.2	100
2	2	neat	6	25	12				372	320	1.2	100
3	3	neat	6	25	>99	702	477	1.5	950	750	1.3	62
4	3	toluene ^d	6	25	>99	583	477	1.2	715	623	1.1	74
5	3	toluene ^d	6	-35	>99	676	548	1.2	769	668	1.2	86
6	3	toluene ^d	6	55	>99	797	529	1.5	1011	704	1.4	62
7	3	toluene ^d	15	-35	>99	1081	781	1.4	1207	1013	1.2	74
8	3	toluene ^d	30	-35	>99	1243	816	1.5	1638	1281	1.3	64
9	4	toluene ^d	6	25	>99	1095	843	1.3	1780	1521	1.2	38
10	4	toluene ^d	15	25	>99	993	811	1.2	1586	1399	1.1	38

^a Conversion of PhSiH₃, determined by the relative intensities of the ¹H NMR signals for the Si-H peaks of the oligomer and the starting PhSiH₃. ^b Molecular weights of the total oligomeric mixture and the linear component, determined by GPC against polystyrene standards. Dividing the M_w and M_n values by 100 gives a rough estimate of the number of PhSiH units in the oligomers. ^c Percent content of the linear portion as determined by ¹H NMR and GPC. ^d 5 M toluene solution.

the Ni-Me complexes (Ni-C(1) ≈ Ni-C(3)) but nonsymmetrical in the Ni-Cl counterparts (Ni-C(1) > Ni-C(3)), reflecting the trans influence order of PR₃ ~ Me > Cl.

To sum up, the spectroscopic and solid-state data indicate that the structures of complexes **1–3** are very similar, the main differences being the slightly longer Ni-P and Ni-Ind distances in complex **2**, which are likely due to the steric bulk of PCy₃. Despite their subtle structural differences, however, these complexes possess very different reactivities toward PhSiH₃, as discussed in the following sections.

Catalytic Results. Addition of catalytic quantities of the Ni-Me complexes to solutions of PhSiH₃ caused an evolution of gas and gave various oligomeric products. The evolved gas was identified as H₂ on the basis of the Raman spectrum of the head gas, which displayed a strong band at 4156 cm⁻¹ corresponding to the literature value for ν(H-H).¹⁸ The consumption of PhSiH₃ and the emergence of the oligomers was conveniently monitored from the ¹H NMR spectra of these reactions in C₆D₆ (PhSiH₃: s, 4.21 ppm; dimer: s, 4.49 ppm; linear oligomers: br, 4.4–4.8 ppm; cyclic (PhSiH)_n: br, 5.2–6.0 ppm).¹³ Studying these reactions under various conditions showed that their rates and final products depend on the precatalyst used and the monomer concentration. Thus, reacting **1** or **2** with 50 equiv of PhSiH₃ (1 M in C₆D₆) led to the slow evolution of H₂ and a gradual formation of the dimer (PhH₂Si)₂ in <5% yields. In contrast, the reaction of **3** with PhSiH₃ under the same conditions resulted in a vigorous effervescence of H₂ and the formation of linear (PhH₂Si)_n oligomers (conversion ca. 95%).

When the catalysis with **1** or **2** was carried out over 6 days in neat PhSiH₃ (ca. 200 equiv), we obtained linear (PhSiH)_n with n = 3–6 (Table 3, runs 1 and 2). The corresponding reaction with complex **3** was much more rapid, giving a virtually quantitative conversion of PhSiH₃ over a few hours to a viscous material that solidified completely over ca. 2–3 days. Analysis of this solid by NMR and GPC showed that it consisted of an oligomeric mixture with a 38:62 ratio of cyclic (n = 5–7) and linear (n = 7–10) components (run 3).¹⁹

The influence of concentration and temperature on the catalysis by complex **3** was studied further with the

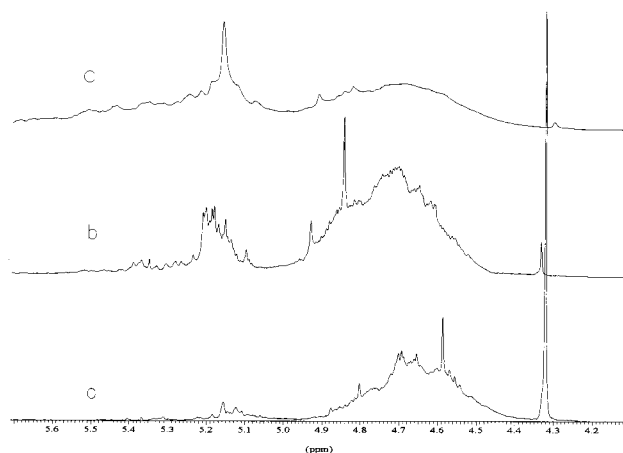


Figure 3. Si-H region of the ¹H NMR spectra for the products of the catalytic runs at -35 °C (a: Table 3, run 5), 25 °C (b: Table 3, run 4), and 55 °C (c: Table 3, run 6).

following results. Somewhat higher proportions of the linear oligomers can be obtained by running the catalysis in concentrated toluene solutions (ca. 5 M) instead of neat PhSiH₃, but the molecular weights of the resultant oligomers are slightly lower (compare runs 3 and 4). Decreasing the reaction temperature to -35 °C did not affect the chain length significantly, but gave more of the linear component (compare runs 4 and 5), whereas increasing the reaction temperature to 55 °C gave longer linear chains and a somewhat diminished linear:cyclic ratio (compare runs 4 and 6; Figure 3). Finally, running the catalysis in concentrated and cold toluene solutions for longer times resulted in much longer linear chains but smaller linear:cyclic ratios (compare runs 7 and 8 to run 5).

Summing up, the oligosilanes obtained from the reaction of **3** display narrow polydispersities (M_w/M_n ca. 1.1–1.5) but lower molecular weights in comparison to samples obtained from some of the best early metal systems such as (Cp)(Cp⁺)ZrCl₂/n-BuLi/B(C₆F₅)₃ (M_w ≈

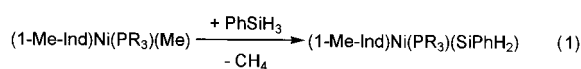
(18) Herzberg, G. *Molecular spectra and molecular structure of diatomic molecules*; V. I. D. Van Nostrand Company Inc.: Toronto, 1950.

(19) To determine whether the mixtures of the oligomeric products contained any poly(hydrophenylsiloxane), which has ¹H NMR chemical shifts similar to those of (PhSiH)_n (ca. 5 ppm in C₆D₆), we recorded the IR spectra of the products. The absence of strong vibrations at 2170 and 1100 cm⁻¹ characteristic of (OSiPhH)_n eliminated this possibility. We have also confirmed (by HMQC ²⁹Si-¹H) that the ¹H NMR signals between 4.4 and 6.0 ppm are correlated to the ²⁹Si NMR resonances in the region of -55 to -65 ppm, which is typical of (PhSiH)_n (ref 13).

3000–14000, $M_w/M_n > 2$ even after multiple fractional precipitations).²⁰ Thus, our results show that the Ni complex **3** and its analogues have the potential to produce high molecular weight polysilanes in contrast to the majority of the previously reported late metal systems, which produce only short oligomers (mainly dimers and trimers).²¹

Mechanistic Studies. A number of interesting mechanistic details on the dehydrogenative Si–Si bond formation catalyzed by our indenyl nickel complexes have emerged from the following experiments.

(1) Analysis of the gas evolved during the early stages of the reactions of the Ni-Me complexes with PhSiH₃ confirmed the presence of CH₄,²² while no trace of PhSiH₂Me was found in the ¹H NMR spectra. This implies the initial formation of a Ni-SiPhH₂ (as opposed to a Ni-H) intermediate (eq 1).



(2) A number of observations have indicated that the formation of oligosilanes begins after only a small portion of the precursor Ni-Me complexes has reacted. For example, the ¹H NMR spectra recorded 30 min after the start of the reaction of complex **3** with 200 equiv of PhSiH₃ showed that some dimer and trimer had already formed, while the only discernible signal in the ³¹P{¹H} NMR spectrum was that of the starting material. For the corresponding reaction with complex **1**, we observed the formation of dimer, while the main P-containing species was the starting material. These results imply that the rate of the initiation step (i.e., the reaction of the Ni-Me precursors with PhSiH₃) is similar to or slower than the subsequent Si–Si bond forming reactions.

(3) The rate of the initial Si–H bond activation reaction between complexes **1–3** and a very large excess of PhSiH₃ (50–90 equiv) at 295 K was studied by monitoring the disappearance of the Ni-CH₃ and the Ind-CH₃ signals of the precatalysts by ¹H NMR spectroscopy. Plots of k_{obs} were linear for complexes **1** and **3**, while the reaction of complex **2** was too slow for convenient measurement. The k_{obs} plots and tables of data are provided in the Supporting Information; these results show that the initial Si–H bond activation proceeds ca. 15 times slower with **1** compared to **3** and much slower still with **2**. Studying the temperature dependence of the reaction of complex **3** between 295 and 339 K allowed the determination of the activation parameters from the Eyring plot (Figure 4): $\Delta H^\ddagger = 10.7 \pm 0.7 \text{ kcal}\cdot\text{mol}^{-1}$ and $\Delta S^\ddagger = -42 \pm 2 \text{ eu}$. The relatively large negative value of ΔS^\ddagger implies a highly ordered transition state for the reaction under study and is

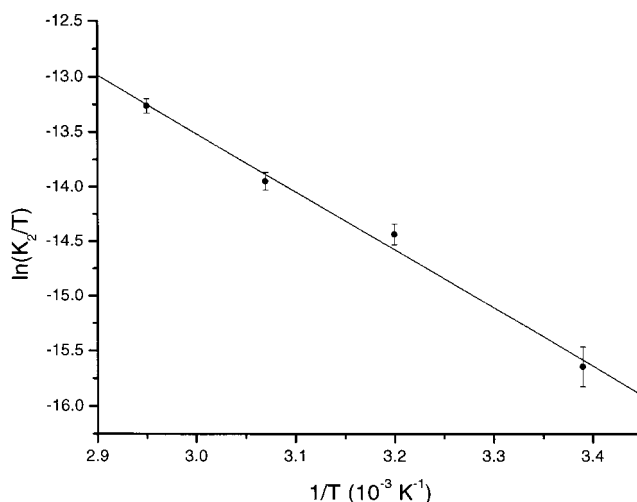


Figure 4. Eyring plot for the reaction of **3** with PhSiH₃. The K_2 values are ($\times 10^{-4} \text{ M}^{-1} \text{ s}^{-1}$): 0.474 ± 0.084 at 295 K; 1.68 ± 0.16 at 313 K; 2.85 ± 0.23 at 325 K; and 5.88 ± 0.33 at 339 K. The activation parameters: $\Delta H^\ddagger = 10.7 \pm 0.7 \text{ kcal/mol}$; $\Delta S^\ddagger = -42 \pm 2 \text{ eu}$.

consistent with the coordination of the Si–H bond to the Ni center²³ prior to the activation step (vide infra).

(4) We have obtained a $k_{\text{H}}/k_{\text{D}}$ ratio of 9.8 ± 0.5 for the reaction of complex **3** with 40 equiv of PhSiD₃ at 313 K.

(5) Monitoring the reaction of **3** with 200 equiv of PhSiH₃ at -30°C by ¹H NMR led to the detection of small amounts of 3-methylindene²⁴ in the reaction mixture after 24 h; no trace of 1-phenylsilyl-3-methylindene was found in this mixture. On the other hand, running the reactions at 325 and 335 K allowed the detection of both 1-phenylsilyl-3-methylindene²⁵ (major) and 3-methylindene (minor). After 24 h, the ¹H NMR spectrum of this mixture showed the formation of the dimer, the trimer, and a number of higher linear oligomers, while the ³¹P{¹H} NMR spectrum showed that the signal for **3** had been replaced by three broad signals at ca. -7.0 , -24.7 , and -25.5 ppm . The first signal is close to those of the complexes (1-Me-Ind)-(PMe₃)Ni-alkyl and might be due to an analogous Ni-silyl or Ni-H species, whereas the more upfield signals appear in the same region as the signals for the Ind-free Ni(0) and Ni(II) complexes (e.g., -21 ppm for Ni-(PMe₃)₄ and -22 ppm for (PMe₃)₂NiCl₂).

The implications of the above observations for the overall mechanism of the dehydrocoupling of PhSiH₃ catalyzed by our complexes are discussed in the next section.

(23) Note that the ligand exchange reaction between PCy₃ and the analogous complex (1-Me-indenyl)Ni(PPh₃)Cl has been found to follow an associative mechanism with the activation parameters $\Delta H^\ddagger = 6.40 \pm 0.04 \text{ kcal}\cdot\text{mol}^{-1}$ and $\Delta S^\ddagger = -40 \pm 4 \text{ eu}$ (ref 8).

(24) From TOCSY and one-dimensional ¹H NMR data (C₆D₆): ¹H NMR (C₆D₆): δ 5.99 (br, 1H, H2), 3.09 (m, 2H, H1), 2.01 (pseudo quartet, $J_{\text{H-H}} = 2.4$, 3H, Me). The aromatic protons were obscured by the much more intense signals due to excess PhSiH₃.

(25) From TOCSY and one-dimensional ¹H NMR data (C₆D₆): δ 6.24 (dq, ³ $J_{\text{H-H}} = 3.7$, ⁴ $J_{\text{H-H}} = 2.1$, ² $J_{\text{Si-H}}$ (for the ²⁹Si satellites) = 160, 1 H, H2), 4.48 (dd, ² $J_{\text{H-H}} = 7.8$, ³ $J_{\text{H-H}} = 2.6$, ¹ $J_{\text{Si-H}}$ (for the ²⁹Si satellites) = 204, 1 H, SiH₂), 4.35 (dd, ² $J_{\text{H-H}} = 7.8$, ³ $J_{\text{H-H}} = 3.1$, ¹ $J_{\text{Si-H}}$ (for the ²⁹Si satellites) = 204, 1 H, SiH₂), 3.56 (m, 1 H, H1), 2.04 (dd, ⁴ $J_{\text{H-H}} = 2.1$, ⁵ $J_{\text{H-H}} = 1.7$, 3 H, Ind-CH₃). The aromatic protons were obscured by the much more intense signals due to excess PhSiH₃.

(20) (a) Gauvin, F.; Harrod, J. F.; Woo, H.-G. *Adv. Organomet. Chem.* **1998**, *42*, 363. (b) Obora, Y.; Tanaka, M. *J. Organomet. Chem.* **2000**, *595*, 1.

(21) Corey, J. Y. *Adv. Silicon Chem.* **1991**, *1*, 327.

(22) Samples of the head gas for the reactions of **3** with large excess of PhSiH₃ were withdrawn using a gastight syringe and injected into a Shimadzu GC-8A gas chromatograph equipped with an Apiezon-L column and an FID detector. The chromatograms thus obtained contained a peak at the same retention time as authentic CH₄ samples.

Discussion

Detailed studies reported by Tilley's group on the polymerization of silanes catalyzed by a family of zirconocene complexes,^{3a} and in particular on the reaction of PhSiH₃ with CpCp*HfCl(SiR₃) (SiR₃ = SiPhH₂^{13a} and Si(SiMe₃)₃²⁶), have shown that the Si–H bond activation and Si–Si bond formation steps involved in these reactions proceed by a concerted, σ -bond metathesis mechanism. In contrast, little is known about the mechanism of the polymerization of silanes by late metals. In principle, low-valent late metal systems are more likely to go through Si–H oxidative addition and Si–Si reductive elimination sequences, whereas σ -bond metathesis type processes commonly occur in d⁰ metal systems wherein oxidative additions are not feasible.²⁷ Nevertheless, it is possible that in some late metal systems the oxidative addition, although feasible, might be energetically less favored than a concerted process. For example, Hartwig has reported that the elimination of methane from the reaction of Cp(PPh₃)₂Ru–Me with H–BR₂ proceeds via σ -bond metathesis.²⁸ We have relied on these literature precedents and the mechanistic findings outlined in the previous section to propose a mechanistic picture for the system under study, as described below.

We propose that the initial reaction between PhSiH₃ and the Ni–Me complexes **1–3** (eq 1) proceeds by a concerted σ -bond metathesis process. The main justification for this proposal is the large kinetic isotope effect found for the Si–H activation reaction by complex **3**. A number of literature reports²⁹ have shown that the oxidative addition of H–H and C–H bonds exhibits k_H/k_D values in the range of 1–2; on the other hand, the concerted, metathesis-type processes often display larger kinetic isotope effects, typically in the range of 2–4,²⁶ but values as high as 10–17³⁰ have also been reported.³¹ The k_H/k_D value of 9.8 ± 0.5 found for the reaction of complex **3** at 313 K is larger than the values of 2.5–2.7 reported by Tilley^{13a,25} for the reaction of PhSiH₃ with CpCp*Hf(SiR₃)Cl at 343 K, but comparable to the value of 9.7 reported by Bercaw et al.^{30a} for the first-order elimination (by σ -bond metathesis) of methane from Cp*Ta(NMe₂)Me₃ at 307 K. Some of the discrepancy between the kinetic isotope effects for the Si–H activation reactions by complex **3** and Tilley's Hf complexes is presumably due to the different temperatures at

which they were measured: the higher temperatures used for the studies involving the Hf systems can be expected to result in higher zero-point energies, which tend to reduce kinetic isotope effects. It appears, therefore, that the kinetic isotope effect for the reaction of complex **3** with PhSiH₃ is in the broad range of the values reported for σ -bond metathesis processes.

Moreover, the ΔS^\ddagger value of -42 ± 2 eu found for our system (vide supra) is also similar to those found for the σ -bond metathesis reactions such as the reaction of Cp*₂ScMe with styrene^{27a} ($\Delta S^\ddagger = -36$ eu) or that of PhSiH₃ with Tilley's Hf compounds mentioned above ($\Delta S^\ddagger = -21$ to -27 eu). Finally, the observation that the rate of the Si–H activation step is very sensitive to steric factors (**3** > **1** >> **2**) is consistent with a highly congested, late transition state typical of a concerted process. Therefore, we propose that the initial Si–H bond activation reactions between PhSiH₃ and the complexes under study proceed by a concerted σ -bond metathesis process. This reaction is believed to generate a Ni–SiPhH₂ species that undergoes subsequent, relatively rapid reactions to form PhH₂Si–SiH₂Ph and higher oligomers; the various pathways that these reactions can follow are considered next.

Since the silyl intermediate does not accumulate in the reaction medium, it could not be detected directly; therefore, we have relied on indirect evidence to determine the sequence of reactions involved in the Si–Si bond formation process. Recall that NMR monitoring of some catalytic reactions led to the detection of 1-phenylsilyl-3-methylindene and PMe₃-containing species which might be Ind-free Ni(0) and Ni(II) complexes (vide supra); these observations hinted at the possibility that the Ni–SiPhH₂ intermediate might undergo a reductive elimination reaction at some point during the catalysis to produce Ni(0) species. To determine whether Ind-free Ni(0) species might play a role in the catalysis, we reacted Ni(PMe₃)₄, **4**, with 200 equiv of PhSiH₃ (5 M in toluene) and observed a vigorous bubbling of gas that continued for a few hours and subsided gradually. Analysis of the viscous oil formed over a few days showed the formation of (PhSiH)_n consisting of 60% cyclic oligomers (Table 3, runs 9 and 10). Taken together, these observations suggest that (a) the Ni–SiPhH₂ intermediate arising from the initial Si–H bond activation step may undergo reductive elimination to give Ind-free Ni(0) species (eq 2), and (b) Ind-free Ni(0) species might be involved in the Si–Si bond forming reactions initiated by precatalysts such as **3** (eq 3).

(26) Woo, H.-G.; Heyn, R. H.; Tilley, T. D. *J. Am. Chem. Soc.* **1992**, *114*, 5698.

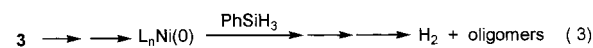
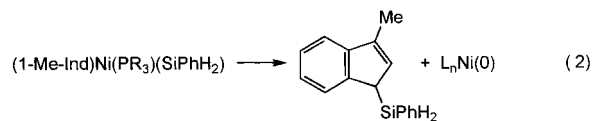
(27) For a discussion of this topic see: (a) Thompson, M. E.; Baxter, S. M.; Bulls, A. R.; Burger, B. J.; Nolan, M. C.; Santarsiero, B. D.; Schaefer, W. P.; Bercaw, J. E. *J. Am. Chem. Soc.* **1987**, *109*, 203. (b) Ziegler, T.; Folga, E.; Bercaw, A. *J. Am. Chem. Soc.* **1993**, *115*, 636.

(28) Hartwig, J. F.; Bhandari, S.; Rablen, P. R. *J. Am. Chem. Soc.* **1994**, *116*, 1839.

(29) (a) Zhou, P.; Vitale, A. A.; San Filippo, J., Jr.; Saunders: W. H., Jr. *J. Am. Chem. Soc.* **1985**, *107*, 8049. (b) Janowicz, A. H.; Bergman, R. G. *J. Am. Chem. Soc.* **1982**, *104*, 352. (c) Collman, J. P.; Hegedus, L. S.; Norton, J. R.; Finke, R. G. *Principles and Applications of Organotransition Metal Chemistry*; University Science Books: Mill Valley, CA, 1987; pp 286–290.

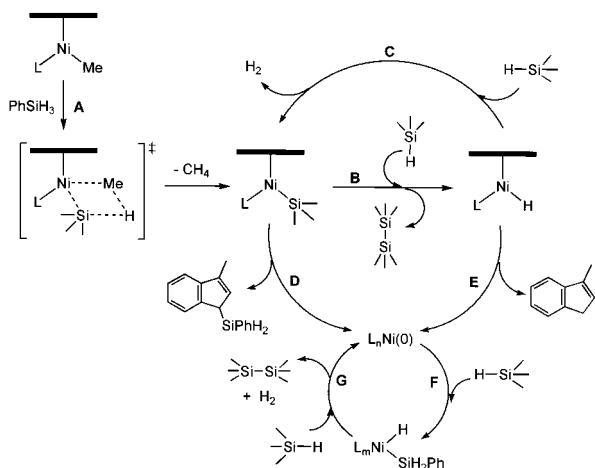
(30) (a) Mayer, J. M.; Curtis, C. J.; Bercaw, J. E. *J. Am. Chem. Soc.* **1983**, *105*, 2651. (b) Hajela, S.; Schaefer, W. P.; Bercaw, J. E. *J. Organomet. Chem.* **1997**, *532*, 45, and references therein.

(31) Unusually large kinetic isotope effects are thought to result from the involvement of quantum mechanical tunneling effects in the rate-determining step: Melander, L.; Saunders: W. H., Jr. *Reaction Rates of Isotopic Molecules*; Robert E. Krieger: Malabar, FL, 1987; p 140.

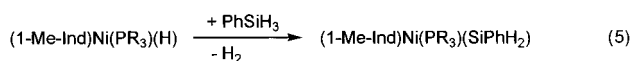
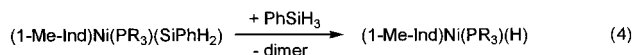


That the above-mentioned reductive elimination of the Ni–SiPhH₂ intermediate is not the only pathway open to this species was inferred from two other pieces of evidence. First, the reactions catalyzed by complex **3** give higher proportions of the linear oligomers compared to those formed from the reaction of **4**. In addition, the

Scheme 1



formation of 3-Me-indene in some of the catalytic reactions initiated by **3**, especially those run at lower temperatures, probably results from the reductive elimination of an intermediate such as (1-Me-Ind)(PMe₃)Ni-H;³² the latter might, in turn, form during a Si-Si bond formation reaction between the (1-Me-Ind)(PMe₃)Ni-SiPhH₂ intermediate and PhSiH₃ or some oligomeric products (eq 4). Therefore, our observations are consistent with a scenario in which the Ni-silyl intermediate follows two pathways: one of these involves a reductive elimination of the silyl and Me-Ind ligands to give a Ni(0) species (eq 2), which catalyzes the dehydrogenative oligomerization of PhSiH₃ to (PhSiH)_n products rich in cyclic components (eq 3); in the second pathway, the Ni-silyl intermediate reacts with PhSiH₃ to give the dimer and an analogous Ni-H species (eq 4), which can, in turn, react with more PhSiH₃ to extrude H₂ and reform the Ni-silyl intermediate (eq 5). The latter pathway appears to be more dominant at lower temperatures (see Table 3, run 5) and gives oligosilanes that are rich in the linear component. The intermediate complexes (1-Me-Ind)(PMe₃)Ni-R (R = H or SiPhH₂) involved in the second pathway eventually follow the reductive elimination pathway to give R-Ind and the Ni(0) species.



Proposed Catalytic Cycle. The above conclusions can be regrouped to develop the tentative mechanistic picture illustrated in Scheme 1. Thus, the Ni precatalysts are proposed to react with PhSiH₃ through a concerted process which releases methane and forms a Ni-SiPhH₂ intermediate (path A). This intermediate is then partitioned into two different pathways, as follows. In path B, the Ni-silyl intermediate reacts directly with PhSiH₃ (or, at a later stage of the catalysis, with a higher oligomer), resulting in the formation of Si-Si

bonds and a new Ni-H intermediate. In path D, the Ni-silyl intermediate undergoes a reductive elimination reaction to produce 1-PhSiH₂-3-Me-indene and generate a Ni(0) species. The Ni-H intermediate generated in path B can then react with PhSiH₃ (or, at a later stage of the catalysis, with a higher oligomer) to extrude H₂ and form another Ni-silyl species (path C). Alternatively, the Ni-H species can eliminate 3-Me-Ind and generate a Ni(0) species (path E).

Finally, the Ni(0) species formed in paths D and E is thought to oxidatively add PhSiH₃ (or a higher oligomer) to generate a new Ni(II) hydrido(silyl) compound which does not bear an indenyl ligand (path F); this species can then react further with PhSiH₃ (or a higher oligomer) to give H₂ and form Si-Si bonds (path G). Although our results do not provide any information on the mechanisms of paths B-E, we suspect that paths B and C proceed via concerted reactions such as that proposed for path A, because the structures of the Ni-silyl and Ni-H species are similar to that of the Ni-Me precursor. Moreover, paths D and E likely involve slippage of the Ind ligand to form η¹-Ind complexes that should be prone to elimination.

The mechanism shown in Scheme 1 combines the reductive elimination and oxidative addition pathways common to late metal systems with the main elements of Tilley's σ-bond metathesis mechanism for Si-Si bond formation by group 4 metallocenes. While some aspects of our proposal are somewhat speculative at this stage, we believe that the results of the mechanistic studies presented here support the main outline of this mechanistic picture.³³ The next stage of our studies will be focused on the preparation of model complexes for the above-alluded Ni-silyl and Ni-H intermediates and studying their reactivities with PhSiH₃.³⁴ We will also study the analogous Cp complexes to determine if the reductive elimination pathway observed with the Ind complexes occurs to the same extent. The results of these studies should advance our understanding of the intimate mechanism of this catalytic process and lead to the development of a new generation of precatalysts with improved features.

Conclusions. The present study has demonstrated that the complexes (Ind)Ni(PR₃)(Me) can act as single-component catalysts for the dehydrogenative oligomerization of PhSiH₃. Since these complexes are generated in situ from the action of MAO on the Ni-Cl derivatives, we conclude that the Ni-Me species are likely involved in the catalysis promoted by the (Ind)Ni(PR₃)(Cl)/MAO system. It should be emphasized, however, that the role of MAO in the latter system is not limited to methylating the Ni-Cl bond; indeed, since the (Ind)Ni(PPh₃)(Cl)/MAO reactions are more rapid and give (PhSiH)_n with higher M_w values than those obtained from the reactions of **1** or **3**,⁶ we believe that MAO plays another, as yet unknown, role in promoting the catalysis.

(32) Since complexes (1-Me-Ind)Ni(PR₃)(X) are stable to hydrolysis, the formation of 3-Me-Ind is unlikely to be related to the residual moisture present in the reaction medium.

(33) A reviewer has suggested that the dependence of the Si-H activation rate on the concentration of added phosphine be measured. Unfortunately, it is not possible to carry out such studies because the presence of excess phosphine (particularly PMe₃) decomposes these complexes, presumably via slippage of the Ind ligand to give (η¹-Ind)Ni(PR₃)_n(Me) followed by reductive elimination.

(34) All attempts to prepare (1-Me-Ind)Ni(PR₃)(X) where X = H, SiR₃ have resulted in decomposition, but PhSiH₃ reacts with the species formed in the mixture of these complexes with LiAlH₄ (ref 6).

Acknowledgment. The authors gratefully acknowledge NSERC (Canada) and Fonds FCAR (Québec) for the financial support of this work; Professor J. F. Harrod for valuable discussions; Prof. X. X. Zhu and his research group for the use of their GPC instrument; and Mr. Ralph Flachsbart from Wilmad Labglass for the gift of the 528-TR-7 NMR tubes.

Supporting Information Available: Complete details on the X-ray analysis of **2** and **3**, including tables of crystal data, collection, and refinement parameters, bond distances and angles, anisotropic thermal parameters, and hydrogen atom coordinates; tables of the raw data for the kinetic studies. This material is available free of charge via the Internet at <http://pubs.acs.org>.

OM010757E